Korean J. Chem. Eng., 38(11), 2217-2228 (2021)
DOI: 10.1007/s11814-021-0879-0

pISSN: 0256-1115
eISSN: 1975-7220

Influence of flow-induced oscillating disturbance on the surface heat transfer of impingement flow

Xiaohang Qu, Xiaoni Qi†, Qianjian Guo, and Yongqi Liu

Department of Energy and Power Engineering, Shandong University of Technology, Zibo 255000, P. R. China
(*Received 24 March 2021 • Revised 10 June 2021 • Accepted 25 June 2021*)

Abstract−Flow-induced oscillation is an effective way to enhance heat transfer, which requires no extra energy consumption and can prevent fouling and soot formation. To test the flow-induced oscillation effect on the heat transfer of impingement flow, an 18 mm wide and 30 μm thick membrane tape was mounted at the exit of the ejection pipe. As the ejection Reynolds number increased from 5280 to 9827, the oscillating frequency also increased. In addition, three different oscillating regimes were observed, these being quasi-still, 2D-oscillating and 3D-oscillating, with the transition *Re* depending on the tape length. The heating plate was 3D-printed and electrical heating wires were embedded within it so as to predetermine the local heat flux by numerical analysis, and be able to calculate the heat transfer coefficient (HTC). The results demonstrate that heat transfer enhancement is more prominent in the vertical direction to the tape than in the parallel direction. Moreover, the distinctive heat transfer enhancement effect near the plate center becomes weaker as it goes toward the outside of the plate, and even turns negative with an increasing r/D. Using a longer piece of tape or having smaller intervals between the tape tip and plate was also shown to improve the heat transfer effect. The spontaneous oscillating disturbance method shows great promise for heat transfer regulation in impingement flow.

Keywords: Flow-induced Oscillating, Heat Transfer Enhancement, Nusselt Number, Impingement Flow

INTRODUCTION

Heat transfer enhancement is a feasible solution for the improvement of energy utilization. Enhancement technology is commonly used and considered an important aspect in industrial production, including in the petrochemical, metallurgical, energy, shipping, aerospace, and machinery fields [1]. Finding ways to enhance heat transfer is a classical problem in the theoretical system and practical application of heat transfer technology. According to its principle, the main physical mechanism of convective heat transfer enhancement can be summarized as follows [2]: (1) Mixing of the fluid, (2) thinning or destruction of the boundary layer, and (3) formation of secondary flow and the intensification of turbulence intensity. Many heat transfer enhancement technologies have been developed, both passive enhancement such as wall fin, tube insert, vortex excitation and turbulence generator, and active ones such as surface oscillation, fluid pulsation, electromagnetic excitation, jet impingement and injection suction.

Fluid-induced oscillation is one type of active heat transfer enhancement technology [3] whose effect has been studied by multiple researchers. In the 1960s, many scientists began studying fluid-induced oscillation, making great breakthroughs in both transverse and longitudinal flow disturbances. In 1964, Bishop and Hassan [4] first proposed the wake oscillation model of flow around a circular tube. Owen [5], meanwhile, proposed a theoretical equation for turbulent buffeting through experimental research. In 1970, Connors proposed a model to solve the problem of fluid-induced oscillation.

To study transverse flow-induced oscillation in heat exchanger tubes, Lam [6] proposed a new fluid structure coupling model based on the surface vortex method. Using this model, the numerical results are able to reproduce the amplitude and nonlinear characteristics of the flow-induced oscillation. The maximum oscillation amplitude and frequency are both in good agreement with the experimental results. With the increase of oscillation amplitude, the amplitude of lift also increases, and the vortex pattern in the near wake also significantly changes. The fluid-induced oscillation of the elastic tube bundle is also successfully simulated through this simple and time-saving method. Zhang [7] pointed out that pulsating flow is an important factor that affects rotor-seal system performance. The nonlinear model of the rotor-seal system with a pulsating fluid flow is established through pulsating flow-induced oscillation. The characteristics of pulsating flow-induced oscillation in the form of sine wave or/and constant flow were quantitatively analyzed based on a Matlab/Simulink numerical simulation. Duan [8] pointed out that by using fluid-induced oscillation, the plane elastic tube bundle's heat transfer efficiency can be enhanced. In this paper, a finite element simulation is used to study the heat transfer characteristics and fluid flows of both the tube and shell sides. Two temperature difference formulae are used to calculate the convective heat transfer coefficient, and the results are verified by theoretical analysis and experimental correlation.

Flow-induced oscillation destroys the thermal boundary layer in the plane elastic tube bundle and enhances the heat transfer. Additionally, due to the influence of having an irregular and complex

†To whom correspondence should be addressed.
E-mail: xiaoniqi@sdut.edu.cn

fluid-flow on both sides of the elbow pipe, the convective heat transfer ability around the two intermediate tube bundles is also enhanced. Khrissy [9] developed a method to measure pipeline flow rates based on the flow-induced vibration principle with water as fluid. Ajayi [10] developed a boundary control method to actively control the angle and fluid-induced oscillation amplitude of an elastic marine riser when under a time-varying distributed load. The torque hydraulic motor is introduced into the upper riser assembly, and the boundary conditions are designed to generate the required signals to control the riser angle and damping, as well as to ensure closed-loop stability. The design is based on the system's partial differential equation and is developed using the energy principle. The program developed within the MATLAB framework was used to arrange the analysis method for the solution. Cheng [11] studied the enhanced heat transfer effect of fluid-induced oscillation with a new type of heat exchange element, which consisted of an elastic tube bundle with a fixed end, an absolute free end and a relatively free end. The results show that compared with the traditional tube bundle, especially when at a low Reynolds number, the enhancement effect achieved with this new type of heat exchange element is very obvious. The in-plane and out-of-plane oscillation of the tube bundle can reduce thermal resistance of fouling by about 20%, which gives great prospects for its use in industrial application.

Judging from existing references, research on fluid oscillation has mainly focused on the heat transfer enhancement of the heat exchanger [12]. From the perspective of structure, most of the above-mentioned heat transfer enhancement technologies belong to the category of fixed oscillation generators, which create vortices by adding fixed structures, so as to enhance convective heat transfer. Many fixed components are needed to achieve an ideal thermal performance for the above. The flexible oscillation generator, meanwhile, can enhance heat transfer by oscillating its flexible body in the channel. This is achieved by the external power system being applied to the generator in order to drive the flexible or elastic body's oscillation and so enhance the transfer of heat. Hidalgo et al. [13] replaced the fins in the vortex generator channel with flexible materials to minimize the pressure drop loss and simplify the heat transfer structure. To enhance the heat transfer, a free-swinging spring was installed in the microchannel of the air-cooled radiator system. Herrault et al. [14], on the other hand, designed a passive swinging spring to enhance heat transfer. Ryu et al. [15], meanwhile, designed a heat dissipation system that uses an inverted flexible flag, discussing its dynamics and what correlation there is between vorticity and temperature distribution.

Jet impingement is an effective method to cool equipment in high temperature environments, and has a wide range of future application prospects for cooling critical machinery structures, such as rocket launchers, turbine blades, modern electronics and compact heat exchangers [16]. However, the technicalities of applying jet impingement to heat transfer enhancement have yet to be fully explored [17]. For example, the conclusions given in [18] and [19] on heat transfer enhancement by impinging jet with a Reynolds number below 10,000 are not consistent. There are two reasons for this: Obtaining an accurate measurement of the convective heat transfer coefficient is very difficult, and the two-equation RANS turbulence model usually overestimates the thermal convection coefficients of the jets [20]. This article will further clarify this confusion. Disturbance-induced flow and heat transfer is a forced coupled convection heat transfer problem. To improve this theory, an experimental method has been developed to study the characteristics of the induced flow and heat transfer of the jets. This method reveals the heat transfer mechanism of the coupled flow between the disturbance and the related variables, and provides guidance for the industrial design and application of heat transfer enhancement technology.

To enhance the heat transfer through fluid structure interaction (FSI), this paper proposes a soft oscillation generator, which has the advantage of having a simple structure and being low cost and energy saving. Oscillation-enhanced heat transfer technology was utilized on the jet impingement. A tape was mounted at the mouth of an ejection pipe to induce the oscillation of the flow. The influence the flutter had on the heat transfer enhancement was then experimentally investigated, with consideration given to factors including the ejection flow rate, height of ejection to plate and the tape-to-plate interval. The temperature and heat flux on each radial location surface was used to obtain the heat transfer's performance. The heat transfer's Nusselt number for impingement flow without the flutter was then validated against an empirical correlation.

EXPERIMENTAL SETUP

1. Facilities and Methods

The experimental loop mainly consists of an air compressor, an ejection pipe, a heating plate, a thermal imager and an oscillating tape, as shown in Fig. 1. Air at room temperature is delivered to the ejection pipe before being impinged vertically onto the heating plate. The ejection pipe is made of PPR with I.D. 22 mm and O.D. 32 mm and a ratio of length to I.D. of more than 60, so the outflow at the pipe exit can be regarded as being fully developed.

To reduce the radial heat conduction and maintain a quasi-constant heat flux on the impingement heating plate, the basic body of the plate with its spiral groove was 3D-printed and made from PLA. The shape and dimensions of the plate can be seen in Fig. 1(a) and (b). The diameter of the plate is 180 mm and the gap between two successive grooves is 5 mm. The cross section of the groove is rectangular and embedded with lead for electrical heating wire. The groove and lead wire both measure 5,141 mm. The plate is mounted on some insulating material to further prevent any heat dissipation from underneath. During the experiment, the wire was heated by a direct electrical current with a total power of 11.5 W, so that a constant internal heat source of 2.85×10^6 W/m^3 could be produced at different radial locations. PLA can greatly reduce the radial conduction, due to its much lower conductivity than lead wire.

To measure the plate surface temperature by non-contact thermal imager, black paint, which is claimed to have an emissivity of 0.95, was coated on both the white PLA and the embedded lead, as shown in Fig. 1(c). The adopted thermal imager is manufactured by Fluke, Inc. Using the same heat plate and black coating as used in the experiment, the thermal imager was calibrated with the readings from the T-type thermocouples. The uncertainty for the temperature range covered in the present study was estimated

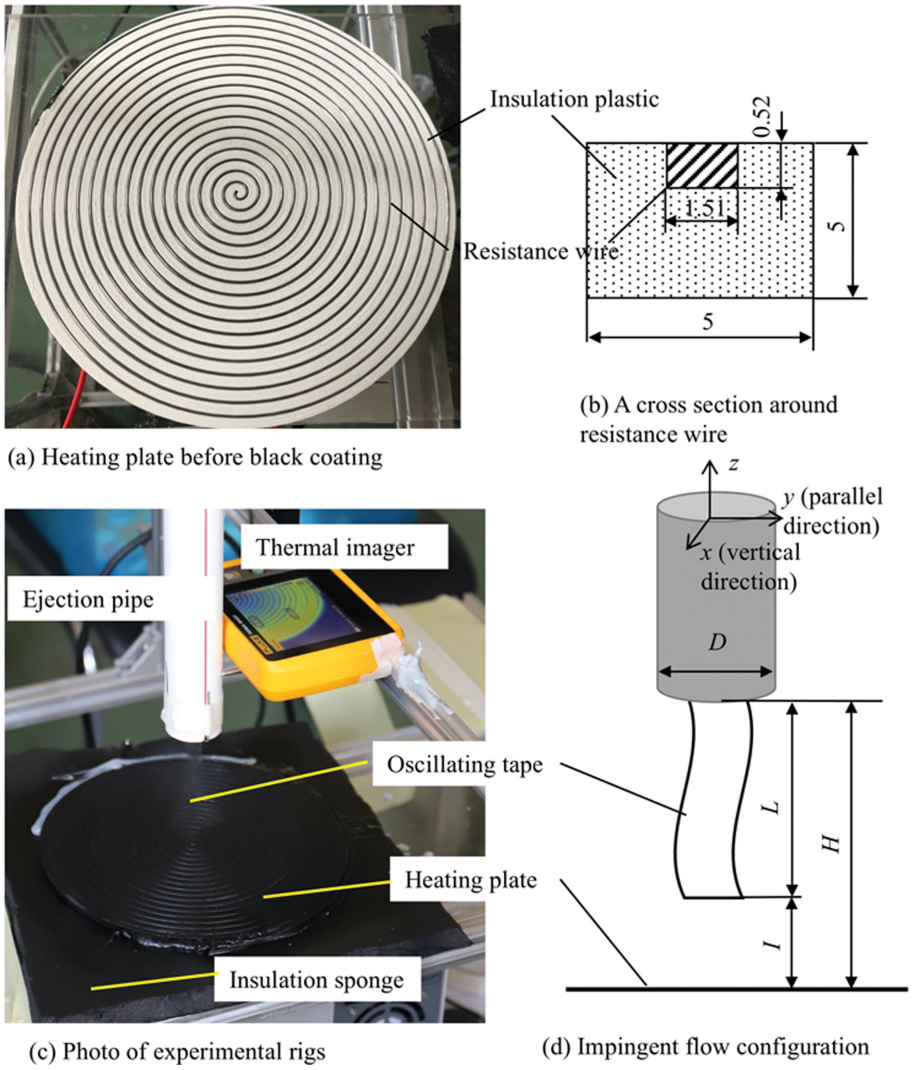

Fig. 1. Experimental rigs.

to be within 0.2 °C.

As shown in Fig. 1(d), the oscillating membrane tape mounted on the exit of the ejection pipe is made from BOPP and has a width and thickness of 18 mm and 30 μm, respectively. The length of the tape is denoted by L and the distance between the pipe exit and plate denoted by H is 65 mm/95 mm. By using different tape lengths, the tape-to-plate interval, I, varies between 5 and 20 mm, which results in a non-dimensional interval I/D between 0.277 and 0.91 along the plate radius. This study mainly shows the variation of the heat transfer performance in two directions, these being vertical to the tape and parallel to the tape, as marked in Fig. 1(d).

The HTC at each radial location where lead is embedded in the plate can be expressed as:

$$h_{ri} = \frac{q_{ri}}{T_{ri} - T_{in}} \tag{1}$$

where q_{ri} is the local heat flux, T_{in} is the room temperature and T_{ri} is the temperature extracted from the measured temperature field in the thermal imager. r_i is the radial distance from the plate center and since the measurement starts from 10 mm away from the center, r_1 equals 10 mm. The average heat transfer performance from the center of the plate to a radial position is an important factor for the application of impingement flow. Therefore, the influence of the oscillating tape on the average Nusselt number is investigated and is defined as [21]:

$$\frac{Nu_{ave}\lambda}{D} = \frac{\Sigma_1^n \pi(r_i^2 - r_{i-1}^2)h_{ri}}{\pi r_i^2} \tag{2}$$

where i is the index of the lead wire and r_0 is taken as zero, h_{ri} is the local HTC on the upper surface of each lead wire at a radial distance r_i defined by Eq. (1), and λ is the conductivity of air. The right term of Eq. (2) is actually an integral part of the local HTC and is expressed in a discrete form, according to the discrete positions of the lead.

2. Uncertainty

To test if a uniform heat flux was obtainable on the top surface of the plate, a pre-simulation was performed on the conjugated head transfer of the zone shown in Fig. 1(b). The boundary condi-

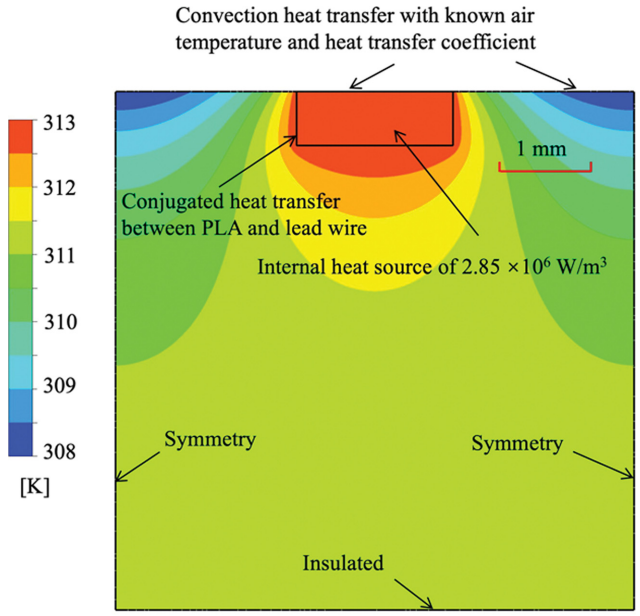

Fig. 2. The pre-simulation of the conjugated heat transfer around the lead wire.

tions and temperature fields are illustrated in Fig. 2, while the heat flux that formed on the top surface of the lead wire at multiple surface HTCs in this study is shown in Table 1. It was found that the surface heat flux varies from 490 W/m^2 to 570 W/m^2 as the surface HTC above the top varies from 30 W/m^2/K to 100 W/m^2/K. This implies that although the PLA base isolates the radial heat conduction in the plate to a great extent, the numerical simulation indicated a surface heat flux variation which depended on an estimated variation range of the local HTC. To conveniently calculate the local HTC for the ejection cases with oscillating tape, a constant heat flux boundary equal to 530 W/m^2 was assumed to be on the lead wire's top surface. In this way, about 8% of the local HTC and Nu uncertainty was produced, and the error was negative for local HTC greater than 60 W/m^2/K (up to −8% for HTC of 100 W/m^{2}K) and positive for local HTC less than 60 W/m^2/K (up to +8% for HTC of 30 W/m^{2}K).

For the present experimental data, the uncertainty was determined by the infrared thermal imager and rotameter's calibration results. The measurement error of the infrared thermal imager was 0.3 k, and the uncertainty of mass flow was 0.2%. The uncertainty of the heat transfer coefficient was calculated according to the error propagation formula described in reference [19]. The maximum relative uncertainty in the Nu is 5.6%.

The resulting flow Reynolds number based on the pipe diameter varies from 5,280 to 9,827 with an uncertainty of less than 5%. For each experimental test run, twenty thermal images were recorded and averaged to obtain the temperature distribution on the plate.

Table 1. The error of heat flux if assuming a constant value of 530 W/m^2

Selected HTC covered (W/m^2/K)	30	45	60	75	90	100
Heat flux on lead surface (W/m^2)	490	511	530	548	565	570
Error if assuming constant	7.94%	3.72%	0.00%	−3.28%	−6.19%	−7.02%

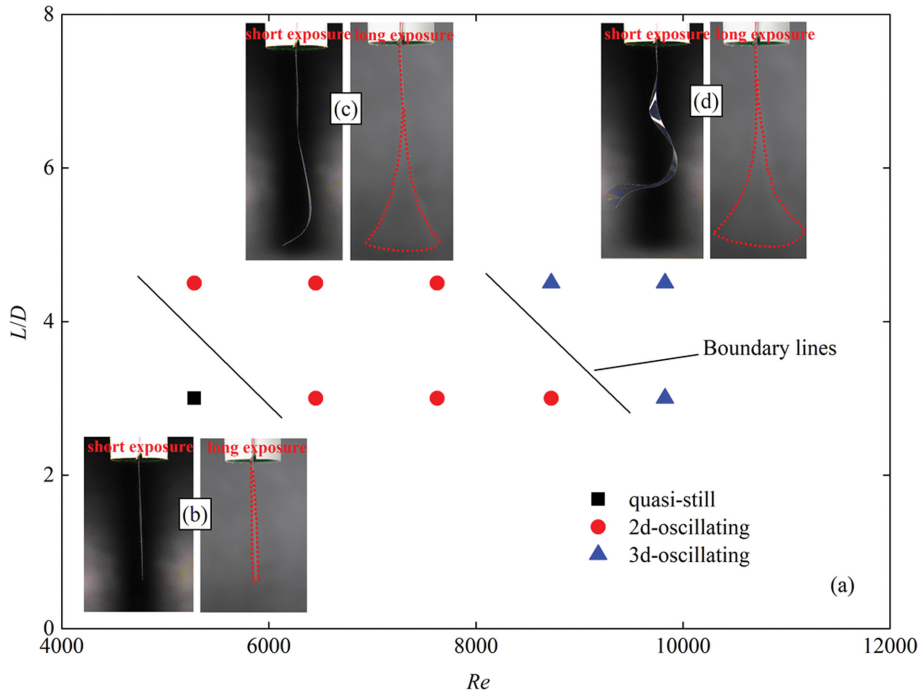

Fig. 3. Tape oscillating regimes at different flow conditions.

RESULTS AND DISCUSSION

1. Flow-induced Oscillation Regime

To obtain an elementary glimpse of the tape's flow pattern under flow disturbance, two image series were taken, as shown in Fig. 3. The first series was taken using a short exposure time and a shutter speed of 1/180 s, within which the instant location and shape of the tape can be freeze-framed. The second series was taken using a long exposure time and a shutter speed of 5 s, from which a qualitative oscillating amplitude and frequency could be obtained. To ensure correct image brightness, the first and second series of images were, respectively, captured using a flash light or neutral density filter.

As shown in Fig. 3, visualization was used to test the tape length variations and ejection flow Re that could affect the oscillating systems. The images taken with short and long exposure are illustrated with boundaries to discriminate between different systems. For a shorter tape measuring 60 mm, three oscillating systems, including quasi-still, 2D-oscillating and 3D-oscillating can be observed, as can an increase in Re from 5,280 to 9,827. It has been speculated that when the flow rate is low and the tape is short, the disturbance transferred to the tape is too small, which only leads to a very faint oscillating frequency and amplitude. With an increase of gas flow rate, increasing energy can be exerted on the tape and a 2D-oscillating tape pattern emerges, as shown in Fig. 3(c). 2D-oscillating, a system which features a curve observed in the parallel direction, as marked in Fig. 1(d), indicates that the flow energy lacks the strength to stimulate the transformation in the tape's width direction, which thus leads to the tape only deforming in a two-dimensional way along the tape's length. When the flow rate is further increased, the higher energy transfer causes deformations at both the length and width directions of the tape, which thus results in a 3D-oscillating system, featuring a three-dimensional surface from the view of the parallel direction, as shown in Fig. 3(d).

A longer tape measuring 90 mm has a larger contact area, which means no quasi-still regimes can be observed and even a small flow rate is able to transfer enough mechanical energy. The Re needed to transition from 2D to 3D-oscillating systems is also lower for longer tape than shorter tape, as indicated by the system's boundary line in Fig. 3. Also, the oscillating frequency increases with the flow rate, as implied by the long exposure images' increased blur with increased Re.

Owing to the oscillating tape's evident directionality, its influence on the heat transfer of the impingement plate needs to be discussed separately, according to the tape's vertical and parallel directions, as shown in subsection 3.4.

2. Qualitative Temperature Distribution

With a 65 mm ejection height H and a 60 mm tape length, the temperature contours obtained from the thermal imager for two flow rates under the influence of the oscillating tapes are shown in Fig. 4. These are compared with those from the non-oscillating tape. Since the heating plate was placed 5 mm below the tape's tip,

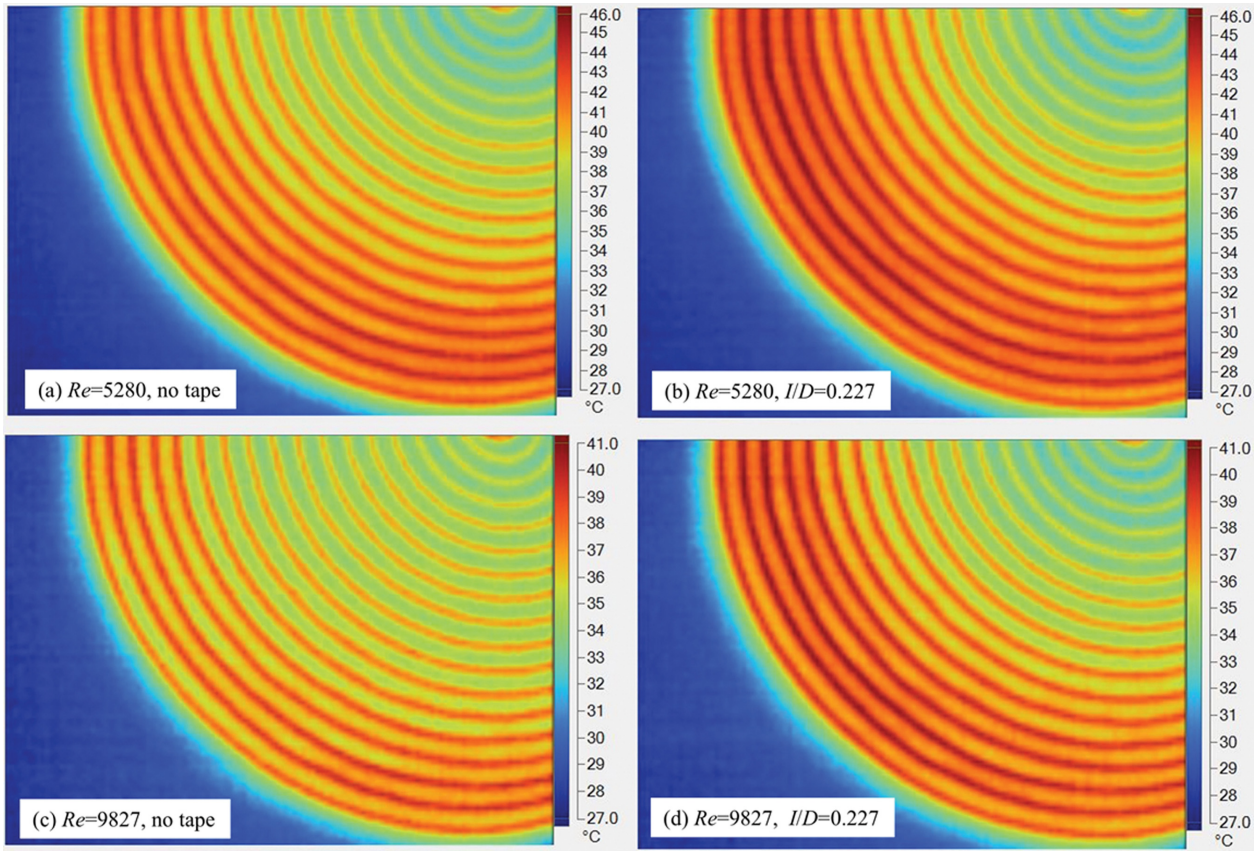

Fig. 4. Variation of temperature distributions with and without oscillating tape (H/D=2.95).

the non-dimensional interval I/D is 0.227. It can be seen from these images that the temperature in the areas where there is lead wire is much higher than locations occupied by PLA. This is because the heat produced by electricity is mainly dissipated through the metal lead. Actually, assuming a constant heat flux for these lead surfaces at different radial locations only generates a heat flux uncertainty of less than 8%, as previously explained in section 3. A higher local HTC under an approximately same heat flux would result in a narrower temperature difference between the surface and the ejected air. Therefore, as the higher impact speed causes an increased local HTC, a lower surface temperature can be observed when the flow Re is higher, as indicated by comparing Fig. 4(a) and (c).

For cases without oscillating tape (Fig. 4(a) and (c)), those locations closer to the plate center will have a lower temperature and higher HTC, which is in accordance with the heat transfer characteristics of impingement flow. However, when tape is mounted at the mouth of the ejection pipe (Fig. 4(b) and (d)), the temperature close to the center becomes lower and the temperature close to the plate rim becomes higher than those cases with no mounted tape. This results in, for the test conditions of Fig. 4 only, an enhanced heat transfer in the middle of an impingement flow and reduced heat transfer at the rim of the plate due to the flow-induced oscillating tape.

To obtain a deep understanding of the factors, including varying tape-to-plate intervals and ejection heights, the discrete distributions of the recorded heat transfer performances are exhibited in the following subsections.

3. Validation of Heat Transfer Measurement

Eq. (3) is an empirical correlation recommended by [22] to predict the averaged Nusselt number of an impingement flow within a round region of r.

$$Nu_{ave}=\frac{h_m D}{\lambda}=2Re^{0.5}Pr^{0.42}\left(1+0.005Re^{0.55}\right)^{0.5}\frac{1-1.1D/r}{1+0.1\left(\frac{H}{D}-6\right)D/r}\frac{D}{r} \quad (3)$$

where the characteristic size for all dimensionless numbers is the pipe diameter D, and the fluid properties are that of the air at the mean temperature of the plate and atmosphere. This equation is adopted here to validate the accuracy of the experimental system and the data reduction procedures described in section 2. Since Eq. (3) is applicable for any r/D larger than 2, only those locations that fit this prerequisite are shown in Fig. 5. The minor deviation of the heat transfer performance between vertical and parallel directions can be attributed to some measurement errors. Based on the analysis carried out at the end of section 3, the positive uncertainty of the experimental data points should be taken into account, meaning that the experimental values are actually below those from the empirical correlation. This is because when calculating the average Nu_{ave} based on Eq. (2), the HTC of the region inside the first measured radial location ($r<r_1$) is taken as the value at the first measure radial location, but this is clearly much smaller than the real value. Nevertheless, it can be concluded from Fig. 5 that the averaged Nusselt numbers at both vertical and parallel directions agree well with the empirical correlations. The reliability of the present experimental methods is further confirmed by the existence of the local HTC's second peak value when the H/D is low and Re is high for the cases without the oscillating tape. This is in agreement with the findings in study [22], as detailed in subsection 3.4.

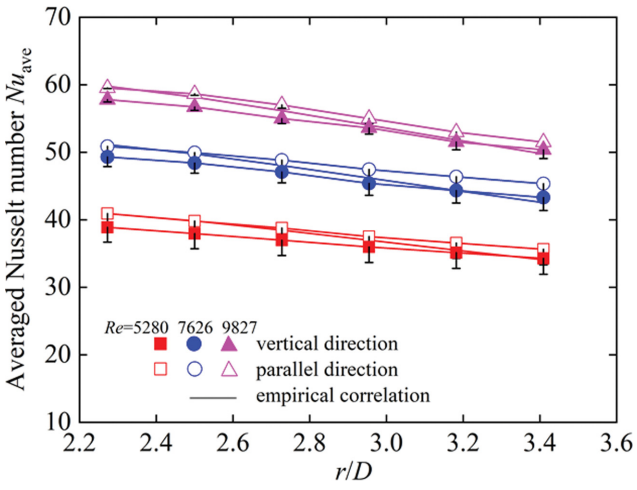

Fig. 5. Validation of the experimental methods.

4. Heat Transfer Performance under Flow-induced Oscillation

As we all know, turbulence can cause strong flow fluctuations, which aids the destruction of the boundary layer and strengthens the heat transfer. Additionally, as reported in reference [23], the jet's oscillation helps improve the overall convective heat transfer performance in the impinging zone. However, other studies [24] argue that the swept jet does not have greater advantages than the static jet impingement for convective heat transfer, especially near the impingement zone. Different studies offer different conclusions, and so this paper will revisit and further clarify this confusion.

Comparing the heat transfer performance of an impingement flow without flow-induced oscillating tape, the local HTC are shown in in Fig. 6 and Fig. 7 for H/D=4.32 and H/D=2.95, respectively. The factors for this comparison include the height of the ejection, the ejection flow rate, the direction relative to the tape (vertical or parallel) and the tape length. It was found that it is the interval (I) between the tap tip, as opposed to tape length (L), that results in the differing heat transfer performance. Therefore, the different line types in these figures represent the variations of the dimensionless interval (I/D). In the present study, one interval (I/D=0.227) and three intervals (I/D=0.227, 0.455 and 0.91) are covered for H/D= 2.95 and H/D=4.32, respectively.

The maximum value of the local HTC emerges at the plate center, and if the ejection height is small and the flow rate is high enough, then a second peak value may also appear. This pattern is well captured by the present measurements for the impingement flow without a tape. For instance, as can be seen from Fig. 6(c) and (f), the Re being 9,827 means that a second peak HTC has emerged at around r/D=2. For a smaller H/D, meanwhile, as expected, the second peak value of the HTC is observed at an even lower flow rate, as shown in Fig. 7(b) and (e), where the Re is 7,626. In contrast, for cases with an oscillating tape, the second peak HTC disappears for all tape-to-plate intervals and the local HTC decreases continuously from the plate center to the rim, as indicated by the

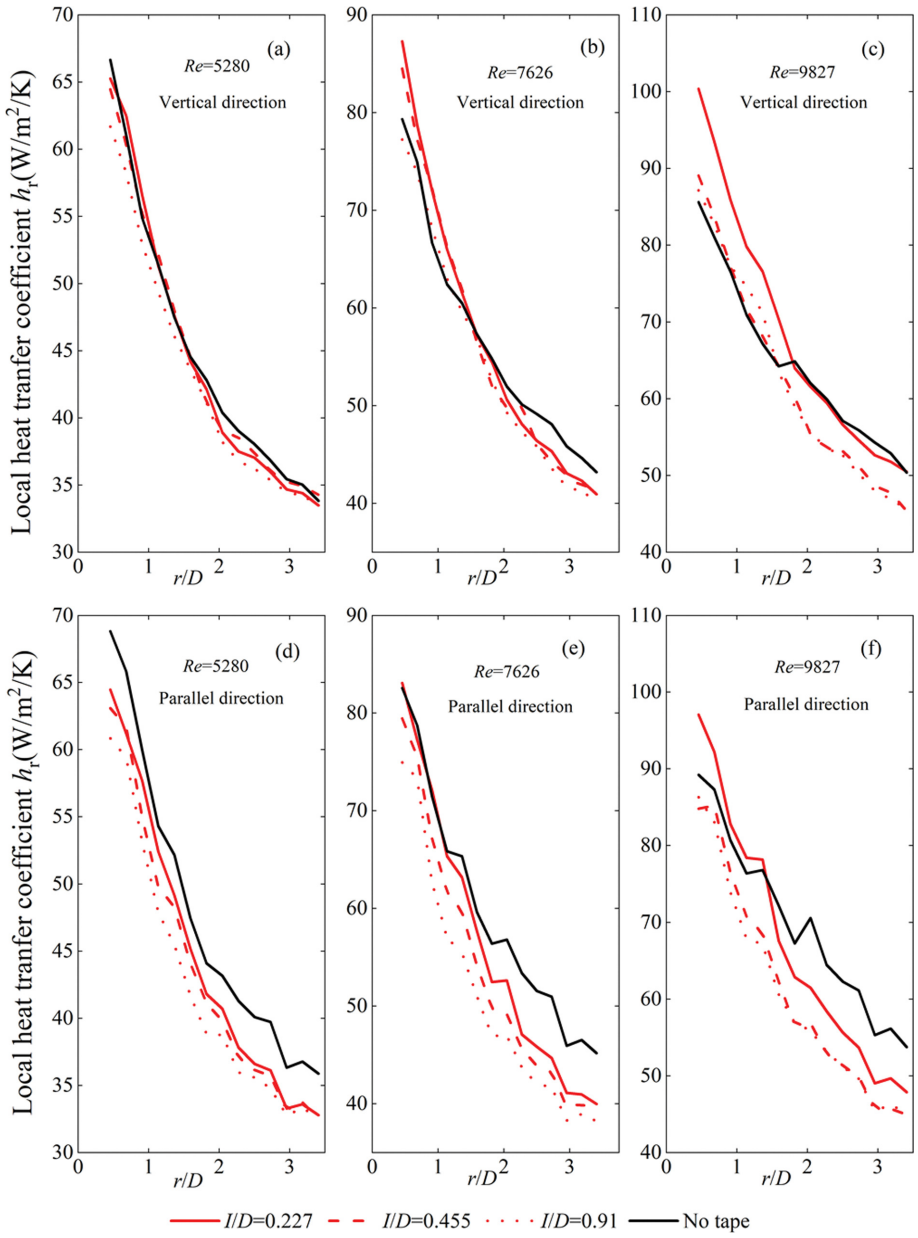

Fig. 6. Distributions of local heat transfer coefficient (H/D=4.32).

red lines in Fig. 6 and Fig. 7. Furthermore, the boundary layer in the central region is thin due to the impact of the jet. With the increase of the radius, a boundary layer gradually develops while the convective heat transfer coefficient decreases. The main reason for the second peak is that the boundary layer develops from a laminar boundary layer to a turbulent boundary layer.

Heat transfer can only be enhanced through the oscillating tape under certain conditions. This can be seen through the comparison of the local HTC with three tape-to-plate intervals at three different Res. This is shown in Fig. 6 where the oscillating tape with the smallest interval results in a higher local HTC than those with larger intervals. As the interval increases however, the difference between the local HTC with different intervals becomes minor. For Re=5,280, no heat transfer enhancement can be observed in the parallel direction, while only a marginal heat transfer enhancement can be observed for the smallest interval (I/D=0.227) in the vertical direction. As the ejection Re increases, both the I/D=0.227 and I/D=0.455 show a local HTC boost in the vertical direction (Fig. 6(b)), while the oscillating tape also starts to show the enhancement effect in the parallel direction, as indicated by the HTC curves for I/D=0.227 and for those without a tape in Fig. 6(e) and (f). For the largest Re that is covered in the present study, the enhancement effect can be observed in all three intervals in the vertical direction, but it is much more pronounced for I/D=0.227 than I/D=0.455 and 0.91. For the ejection height H/D=4.32, a maximum enhancement ratio of 18% can be obtained at Re= 9,827 and I/D=0.227, as shown in Fig. 6(c).

Distributions of the local HTC for a lower ejection height H/

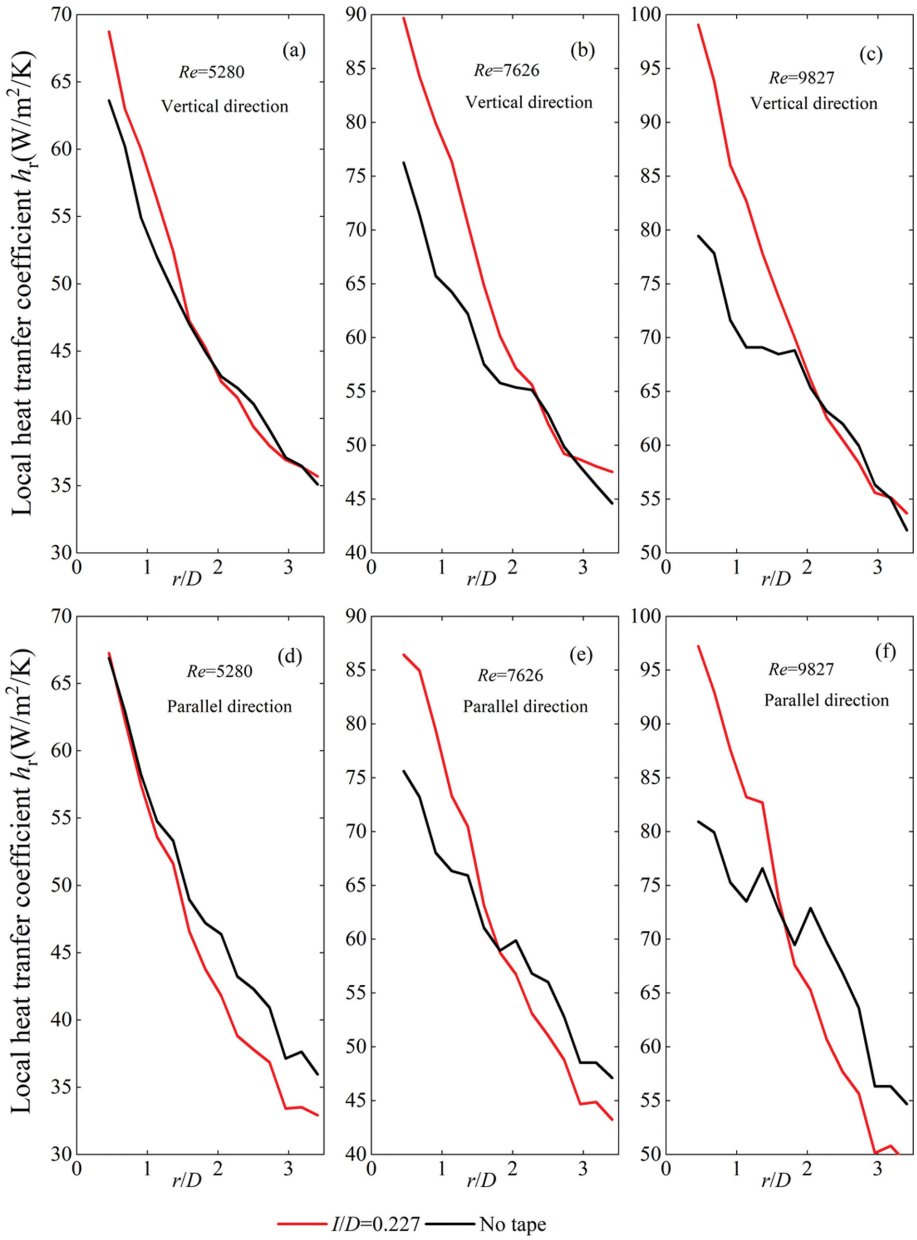

Fig. 7. Distributions of local heat transfer coefficient (H/D=2.95).

D=2.95 are illustrated in Fig. 7 and since the HTC boost is found to be indistinctive for cases with a larger tape-to-plate interval, only an interval of I/D=0.227 is included. In order to vary the extent for all flow Res in both the vertical and parallel directions, the local HTC can be enhanced by the tape. When comparing Fig. 6 and Fig. 7, it can be concluded that for lower H/D, a larger enhancement ratio of the local HTC can be reached and this ratio can be as high as 25%.

Meanwhile, a local HTC boost over the impingement flow without a tape only occurs from those zones in close proximity to the plate's center and as far as certain critical radial locations (denoted as r_c). Beyond these critical locations, however, the boost effect vanishes. The existence of these critical locations indicates that the local heat transfer enhancement effect produced by the flow-induced oscillating tape can at some point transform into a heat transfer reduction. In addition, the critical location r_c/D is also found to increase with the ejection flow rate. For instance, in Fig. 6(b) and (c), as the Re increases from 7,626 to 9,827, the r_c/D goes from less than 2 to larger than 2, while in Fig. 7(a) to (c), as the Re increases from 5,280 to 9,827, the r_c/D increases from 1.5 to about 2.2. Meanwhile, the jet with tape disturbs the stagnation zone and results in an increase of the vortex intensity in the flow space, an enhancement of the fluid scouring ability on the wall in the central region, and the enhancement of the heat transfer ability in the stagnation zone. Due to the limited disturbance region, the heat transfer coefficient that is far removed from the stagnation region shows little difference.

Over a zone with a radial distance lower than r, the local HTCs

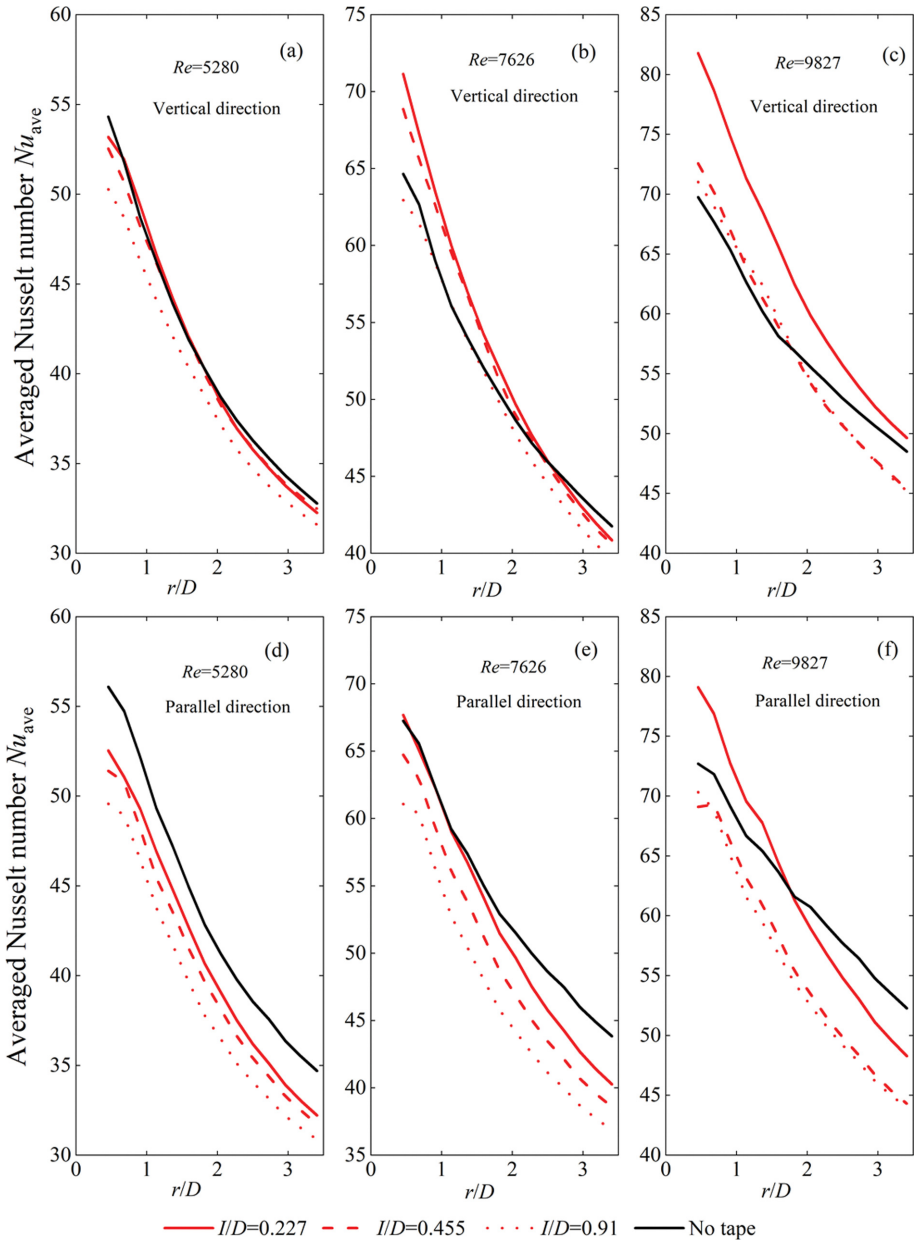

Fig. 8. Distribution of averaged Nusselt number for a zone inside r/D (H/D=4.32).

are processed by Eq. (2) and the averaged Nusselt numbers Nu_{ave} are obtained with the results for H/D=4.32 and H/D=2.95, which are shown in Fig. 8 and Fig. 9, respectively. As expected, the Nu_{ave} also exhibit huge values when close the plate center and decrease as they move towards the plate rim. Similar to the trend for the local HTC, the shorter the tape-to-plate interval, the easier it is to obtain a Nu_{ave} boost when at small Re. As shown in Fig. 8(a), for Re=5,280, only a slight boost of Nu_{ave} emerges for I/D=0.227 in the vertical direction. As the ejection Re increases to 7,626, the boost appears for I/D=0.227 and 0.455 in the vertical direction (Fig. 8(b)) and for I/D=0.227 in the parallel direction (Fig. 8(e)). When the ejection Re reaches 9,827 meanwhile, the Nu_{ave} enhancement effect can be observed for all three intervals in the vertical direction and for I/D=0.227 in the parallel direction. When comparing Fig. 9 to Fig. 8, the Nu_{ave} boost appears to be more prominent for a shorter ejection height of H/D=2.95 than for the higher H/D=4.32. This is consistent with the local HTC distributions, as show in Fig. 6 and 7.

Since the Nu_{ave} were calculated by integrating the HTC through a zone within a radial distance of r from the plate center, the critical radial location where the Nu_{ave} were produced by the oscillating tape goes down below the Nu_{ave}, while without a tape it is postponed to a further distance than the critical location of the local HTC. For instance, for Nu_{ave}, the r_c/D for the local HTC shown in Fig. 6(b) was postponed from 1.8 to 2.6 in Fig. 8(b). The r_c/D for the local HTC shown in Fig. 7(f), meanwhile, was also postponed for Nu_{ave}, from around 2 to 2.5 in Fig. 9(f). Moreover, for those cases where local HTC has been enhanced to a great extent,

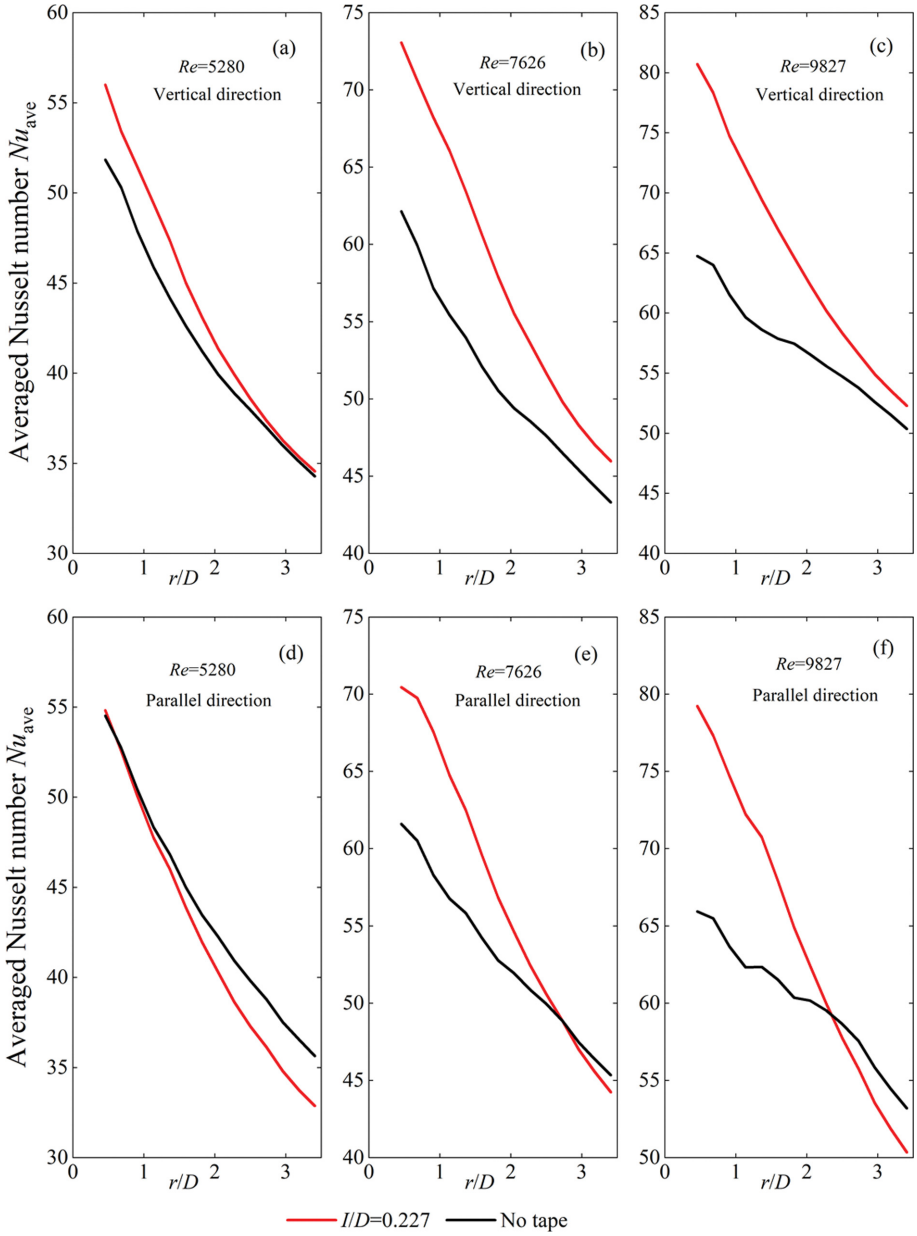

Fig. 9. Distribution of averaged Nusselt number for a zone inside r/D (H/D=2.95).

such as in Fig. 6(c), and Fig. 7(b) and (c), the flow-induced oscillating tape results in Nu_{ave} being larger than those without a tape for the whole radial locations of the impingement plate, as was seen in the I/D=0.227 curve of Fig. 8(c), and Fig. 9(b) and (c). The small impact height H means that the core area of the jet is larger, so the impinging jet has more kinetic energy. In addition, due to the large pressure gradient near the impact point, the jet is in a state of acceleration. The wall jet then flows around and disturbs the surrounding media. During the momentum exchange process, the wall jet decelerates gradually and the viscous boundary layer on the wall gradually thickens; the larger the kinetic energy in the core region of the jet, the smaller the thickening range of the boundary layer.

5. Discussion

One of the most effective ways to use jet impingement to enhance heat transfer is to excite and change the flow state of the fluid. Based on the quantitative results on temperature distribution and the heat transfer coefficient, it can be established that the influence of the flow-induced oscillating tape on the impingement flow's heat transferring performance is two-sided. According to these observations, the flow pattern under the disturbance of the oscillating tape can be schematically illustrated, as shown in Fig. 10. As expected, no matter whether the fluid is close or far from the center line, the oscillating tape is able to disturb the flow that is ejected from the nozzle. However, since the impingement flow in the present study is unconfined, the instantaneous curved tape can reflect a small portion of the fluid away from the surface of the plate and then stop it from returning back to the plate. Therefore, the stream that is close to the center of the plate can be more effectively dis-

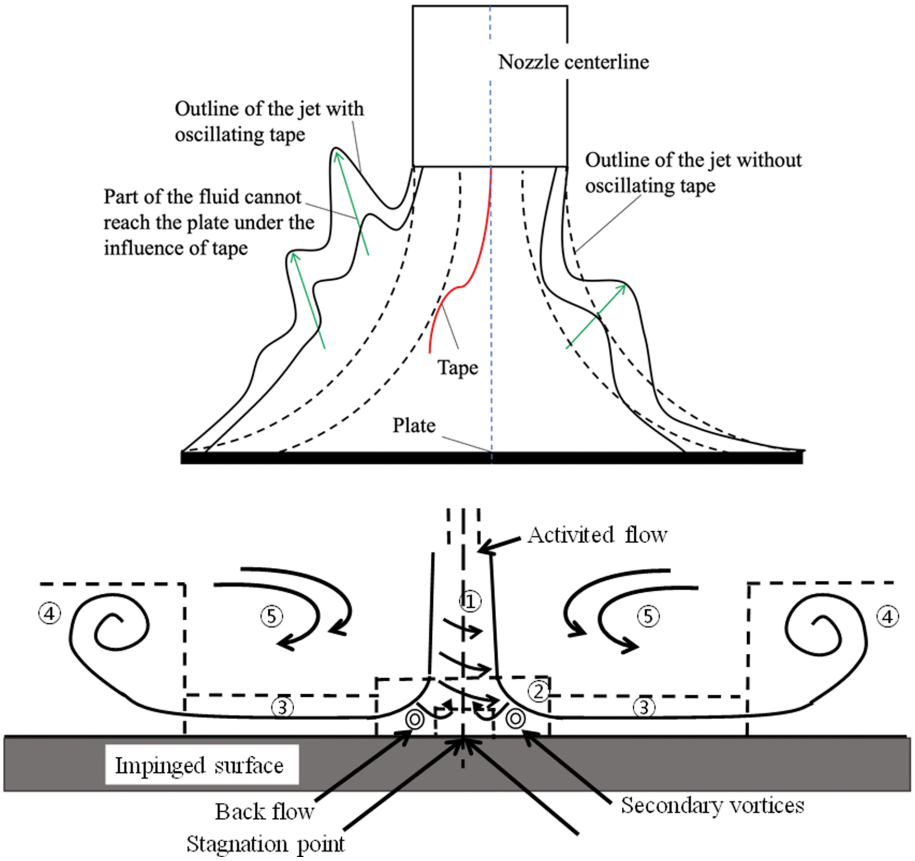

Fig. 10. Illustration of the flow pattern under the influence of oscillating tape.
① Free jet ② Impinged area ③ Inspired flow mixing ④ Flow separation ⑤ Entrainment ⑥ Internal flow mixing

turbed by the tape, the reflection effect is weaker and the heat transfer performance can be improved. For the stream around the perimeter, however, the turbulence produced by the tape in the center becomes weaker and the reflection of the fluid decreases the flow velocity, which means that the heat transfer performance will deteriorate. This indicates that disturbance tape can effectively change diffusion velocity, turbulence intensity and boundary layer distribution. Jet impingement with oscillating disturbance produces a huge eddy current, which leads to an unstable boundary layer on the target plate. There being a high or low heat transfer rate, meanwhile, mainly depends on the jet frequency, the size of the tape and plate, and the jet Reynolds number: parameters that increase the complexity of the fluid flow, especially in the jet interaction zone. Jet impingement with disturbing technology is characterized by having a high turbulence intensity, unstable fluid flow, effective chaotic mixing and a nonlinear dynamic response of the thermal dynamic boundary layer, which can improve heat transfer efficiency. The results show that the flow velocity's non-uniformity, which is caused by tape, greatly influences both flow and thermal performance during the impact process.

The enhanced heat transfer of the disturbed jet depends on its application, due to the jet pulsation's destruction of the boundary layer on the hot surface. This happens because the pulsating energy in the downstream region of the jet is sometimes uselessly consumed during the formation of the flow vortex structure. For tape, the control parameters of the flow field can be divided into geometric parameters, driving parameters, jet to surface distance, tape length and width. How effective the heat transfer enhancement is mainly depends on the streamwise vortex's ability to hold out for a certain distance in the wake region. The internal region disappears due to the limitations posed by the potential core range, while the coherent vortex structure also has an effect on the enhanced heat transfer. However, there is no disturbing jet design to suit a variety of geometric structures. Thus, further work is still required to better understand the physical mechanism behind heat transfer enhancement by interference jet. This further work will help to identify an effective flow field management system, which will in turn produce more effective heat transfer enhancement methods.

CONCLUSION

The influence that disturbance has on the heat transfer characteristics of impingement flow was experimentally investigated in the present study, with the factors considered including the ejection flow rate, the height of ejection to the plate and the tape-to-plate interval. The main conclusions are:

(1) The oscillating system can be classified into quasi-still, 2D-oscillating and 3D-oscillating. It is therefore expected that an oscillating tape's influence on the heat transfer of the impingement flow can be related to whether the measurement direction is vertical or

parallel to the tape.

(2) Not every oscillating tape configuration enhances heat transfer performance. For the flow Reynolds numbers and the tape dimensions covered in the present study, for example, heat transfer enhancement was only obtainable when in the region close to the plate's center for small tape-to-plate intervals, short ejection heights to plate and high ejection flow rates. In the present study, the maximum improved heat transfer ability over the impingement flow without a tape was 25% and 18% for H/D=2.95 and 4.32, respectively.

(3) A critical radial position exists, beyond which point the oscillating tape functions only to worsen the heat transfer performance. This critical position increases with the increase of the ejection flow rate.

(4) The present study demonstrates that spontaneous oscillating tapes are very promising for the regulation of the heat transfer of impingement flow. In addition, the detailed experimental data that has been gathered can be used for CFD validation. In order to propose empirical corrections for practical application, future research should be devoted to exploring wider flow parameters, especially the dimensions of the oscillating tape.

ACKNOWLEDGEMENTS

The authors would like to extend their sincere gratitude to National Natural Science Foundation of China (51806128 and 51879154), Natural Science Foundation of Shandong Province (ZR2019BEE008 and ZR2019MEE007) and China Postdoctoral Science Foundation (2020M682211).

REFERENCES

1. A. Sadeghianjahromi and C.-C. Wang, *Renew. Sust. Energ. Rev.*, **137**, 110470 (2021).
2. R. L. Webb, *Principle of enhanced heat transfer*, Wiley, New York (1994).
3. S. Ghanami and M. Farhadi, *Protein Sci.*, **7**(1), 9 (2019).
4. R. Hassan, *P Roy Soc Lond A Mat*, **277**(1368), 51 (1964).
5. P. R. Owen, *J. Mech. Eng. Sci.*, **7**(4), 431 (1965).
6. K. Lam, G. D. Jiang, Y. Liu and R. So, *Int. J. Numer Methods Fluids*, **46**(3), 289 (2004).
7. N. Zhang, *Adv. Mat. Res.*, **542-543**, 66 (2012).
8. D. Duan, P. Ge and W. Bi, *Energy Convers. Manag.*, **103**, 859 (2015).
9. K. A. R. Medeiros, F. L. A. de Oliveira, C. R. H. Barbosa and E. C. de Oliveira, *Measurement*, **91**, 576 (2016).
10. O. O. Ajayi, M. C. Agarana and T. O. Animasaun, *Procedia Manuf.*, **7**, 602 (2017).
11. L. Cheng, T. Luan, W. Du and M. Xu, *Int. J. Heat Mass Transf.*, **52**(3), 1053 (2009).
12. M. H. Mousa, N. Miljkovic and K. Nawaz, *Renew. Sust. Energ. Rev.*, **137**, 110566 (2021).
13. P. Hidalgo, F. Herrault, A. Glezer, M. Allen and B. S. Rock, *Thermal Investigations of ICs and Systems (THERMINIC)*, 2010 16th International Workshop on (2010).
14. F. Herrault, P. A. Hidalgo, C. Ji, A. Glezer and M. G. Allen, *2012 IEEE 25th International Conference on Micro Electro Mechanical Systems (MEMS)*, 1217 (2012).
15. J. Ryu, S. G. Park, B. Kim and H. J. Sung, *J. Fluids Struct*, **57**, 159 (2015).
16. G. Krishan, K. C. Aw and R. N. Sharma, *Appl. Therm. Eng.*, **149**, 1305 (2018).
17. L. Yong and M. C. Xiao, *Eur. J. Mech. B Fluids*, **57**, 40 (2016).
18. L. Agricola, R. Prenter, R. Lundgreen, M. Hossainf and J. Bons, *53rd AIAA/SAE/ASEE Joint Propulsion Conference* (2017).
19. T. Park, K. Kara and D. Kim, *Int. J. Heat Mass Transf.*, **124**, 920 (2018).
20. M. Germano, U. Piomelli, P. Moin and W. H. Cabot, *Phys. Fluids A*, **3**(7), 1760 (1991).
21. P. Chorin, F. Moreau and D. Saury, *Int. J. Therm. Sci.*, **161**, 106711 (2020).
22. M. Holger, *Adv. Heat Transf.*, **13**, 1 (1977).
23. C. Camci and F. Herr, *Int. J. Heat Mass Transf.*, **124**(4), 770 (2002).
24. M. A. Hossain, L. Agricola, A. Ameri, J. W. Gregory and J. P. Bons, *2018 AIAA Aerospace Sciences Meeting* (2018).